

UNIVERSITY OF SOUTHERN CALIFORNIA
School of Medicine
2025 Zonal Avenue
Los Angeles, California 90033

NASA CR 107187

Department of Physiology

24 November 1969

NASA CONTRACT NO. NSR 05-018-087

PROGRESS REPORT:

Period covered: July 10, 1969 to October 9, 1969

ABSTRACT

During this reporting period the major efforts were concentrated toward developing an implantable cardiac sonomicrometer. Circuitry was designed and tested, several crystal probes were fabricated and the device was calibrated and tested by an acute measurement of dynamic atrial and vena cava dimensions in an experimental animal.

CASE FILE COPY

DISCUSSION

The dimension of certain organs is often important in determining the response of a subject to a particular environment. Examples include the dimensional change in cardiac structures as a result of mechanical stresses and splanchnic contraction during hemorrhage. A less quantitative change occurs in central venous volume and thus the dimensions of the encompassing structures when test subjects are immobile for long periods, immersed in water or subjected to weightlessness. The determination of dynamic volume changes associated with these environments has generally been by the indirect means of measuring the pressure change and estimating volume changes by reference to experimentally determined pressure volume curves. The structures bounding this volume are typically quite compliant with the result that in low pressure areas a small change in pressure produces a large change in volume. The compliance in the venous system is on the order of one liter/mmHg. It is evident that a reasonable determination of volume change necessitates a rather exact determination of pressure. Measurement of the pressure under mobile conditions is not a simple task and may not be sufficiently accurate to predict volume changes. An unrelated problem is that of adaptation of the structure to modification in internal pressure. It is likely that a prevailing high pressure would result in expanding structures and a consequent decrease in pressure. Without knowledge of the dimension it cannot be determined if the decreasing pressure was caused by structural expansion or a decrease in the quantity of fluid. This quandry can be avoided if both pressure and dimension are measured since the volume is a function of dimensions and dimension is a function of the internal pressure and the tone of the bounding structure.

Cardiac dimensions have been measured by transducing techniques varying from capacitance to X-ray. The ultrasonic technique presented in this paper has the merit that it approaches a digital technique depending on the transit time between two displaced crystals. Time invariant transducer properties are not an absolute requirement to obtain stable electronic operation so long as the crystals will respond to electrical and mechanical energy sufficiently to cause initiation of pulsed information. The transmitting crystal can be overdriven to insure sufficient transmission of energy while the electronics on the receiving crystal can be endowed with excessive gain to insure adequate pickup under most circumstances.

24 November 1969

-2-

It can be appreciated that unless the volume being measured has well defined boundaries and only one dimensional change, then the detection of only one dimension is insufficient to describe the volume. The measurement of volume of cylindrical structure is perhaps more feasible since the volume is related directly to the diameter if the length is assumed constant. The measurement of structure such as the atrium and ventricle by linear dimension cannot yield an absolute volume but only an indication.

The concept of employing the transit time of ultrasonic energy from a transmitting to a receiving crystal as a means of measuring distance is not new. This technique has been employed by several workers in cardiovascular dynamics. They have not generally concerned themselves with miniaturization and conservation of power to an extent which adapts their device for long term implants in small animals. Our efforts have therefore been directed toward modifying and extending existing concepts in order to produce an improved version of an existing device which will be feasible for long-term implants.

Figure 1 is a block diagram illustration of a technique employed by workers at the USAF School of Aerospace Medicine (1). The broad concept is to electrically excite a transmitting piezo-electric crystal producing mechanical oscillations and measure the time required for the receiving crystal to respond with sympathetic mechanical vibrations. This time is proportional to the transit time which is in turn proportional to the distance between crystals. The illustration in Figure 1 displays in block form the electronics required to excite the transmitting crystal, detect the resonant vibrations of the receiving crystal and to measure the time for energy transit in order to obtain a measure of distance. The "pinger" strikes the transmitting crystal with a very sharp pulse, initiating mechanical vibration at 5 MHz. The pinger also sets a monostable circuit which is adjusted to reset after several μ seconds. In resetting, it sets a bistable circuit. If the bistable is set by the pinger without a delay, it is immediately reset by the capacitive coupling from transmitting to receiving crystal. The monostable delays the set of the bistable until the capacitive interference has dissipated. The energy detected at the receiving crystal, which is delayed by the transit time, produces an electrical output at the crystal. This signal is amplified and used to reset the bistable. The bistable output is thus a rectangular output with width equal to the acoustical delay between the crystals less the on time of the monostable. Proper conditioning of this pulse produces a voltage proportional to the distance. The duration of the capacitive coupled energy limits the minimum distance which can be measured. Since the velocity of the ultrasonic energy in biological structure is about 1.55 mm and the electronic delay on the monostable is set to μ sec

2 μ sec to avoid the capacitive interference problem the minimum distance measurable is approximately 3 mm.

ELECTRONIC CIRCUIT

Figure 2 illustrated a circuit for an operational sonomicrometer. The pinger in this case consists of a free running pulse generator which produces 2 μ second pulses at a one KHz rate. The rate is controlled by time constant $R_1 C_1$ and the duration by $R_3 C_2$. When the voltage at the cathode gate of SCS₁ reaches the triggering level, normally about .7 volt, SCS₁ conducts and the supply

voltage less the forward voltage drop of the SCS appears across R_4 . Capacitor C_2 then starts to charge, turning on Q_1 and lowering the voltage applied to the cathode gate. When Q_1 is sufficiently on, capacitor C_1 discharges and the SCS₁ is turned off.

Transistor Q_2 is a pulse shaper converting the pulse from the SCS output to a negative pulse with V_{max} of 9 volts and a rise time from 10-90% of 50 nanoseconds, a fall time from 90-10% of 80 nanoseconds, a 90% pulse width level of 80 nanoseconds and a 10% level of 260 nanoseconds. With these conditions the pick-up level on the receiving crystal at 20 mm is approximately 20 mv.

When the pinger turns on it also sets the monostable consisting of SCS₂. When the monostable resets it sets the bistable and turns on transistor Q_5 and applies power to the R.F. amplifiers. The bistable is then reset by the received signal producing a pulse width proportional to the distance between crystals. When the bistable resets it also turns Q_5 off, removing power from the two 703 RF amplifiers. The control of power to the R.F. amplifiers saves considerable current as each 703 draws about 5 ma at 10 volts while the remaining circuitry draws very little. With this technique the average current is approximately 1 ma when the distance between crystals is 100mm. A D.C. voltage proportional to the distance is obtained by passing the output of the bistable through the low pass filter. Figure 3 illustrates the calibration curve for the device; for a linear output the sensitivity is approximately 5 mv/mm.

TEST RESULTS

To test the feasibility of the unit, tests were made on one dog. Figures 4 and 5 illustrate the results. Figure 4 is a tracing of dimension change obtained across a portion of the right atrium. The crystal probes were sutured to a nearly transverse wall of the atrium and connected to a breadboard circuit. The absolute dimension was lost in expanding the scale in order to improve the resolution of the dimension change. Figure 5 is a similar tracing obtained across the anterior vena cava. The dimension change was on the order of 1.4 mm.

FUTURE CONSIDERATIONS

In terms of optimization of this circuitry, several things appear feasible. Since in a rough consideration it would appear that in considering similar tissue being expanded by equal pressure, the dimensional change would be roughly proportional to the absolute dimension. Thus the relationship between dimension and pressure is a log function that is:

$$D = K_1 e^{KP}$$

An instrument designed to measure this change would thus require greater resolution when the measurement is being conducted on an organ with small dimensions. Improvement in the resolution of measurement can be achieved by proper design of the output filter as shown in Figure 6. From the knowledge that the velocity of sonic energy in tissue is approximately 1.55mm per μ second and that the maximum dimension desired to measure is 100mm, we arrive at a maximum pulse width from the output of the bistable of 65 μ seconds. If the time constant $R_1 C_1$ is on the same order of the pulse width, the output voltage on C_1 will vary nonlinearly with the pulse width, the time constant $R_1 C_1$ can be selected as 32.5 μ seconds

producing an output voltage on C_1 equal to 63% V_{max} when a 32.5μ second pulse is applied to the input. The voltage on C_1 in terms of time is defined by

$$e_1 = V_{max} (1 - e^{-t/R_1 C_1}).$$

Since $t = D/1.55$, $\frac{t = D}{1.55} \text{ sec}$ and $R_1 C_1 = 32.5$ seconds, it can be written that

$$e_1 = V_{max} (1 - C_2^{-D/50}).$$

The sensitivity is then $\frac{de_1}{dD} = \frac{V_{max}}{50} C^{-D/50}$.

At $D=0$ and $V_{max} = 10$ volts, the sensitivity is 200 mv/mm and at $D=100$ mm, the sensitivity is 26 mv/mm. Over the linear output on the small dimensions an increase of 40 is obtained and in the larger dimension a factor of 5 is obtained, all at no expense in system stability.

Inspection of an actual calibration curve as illustrated in Figure 6 reveals that linearity can be assumed for limited dimensional changes. Thus if one first uses the given curve to find the nominal dimension, a new equation can be written using the known dimension and the slope of the curve at that point.

PROBE FABRICATION

The first probes were crystals mounted on a thin slab of polystyrene. Difficulty was encountered in attaching to and maintaining alignment on the cardiac surfaces. It can be concluded that the alignment will be difficult to achieve due to the typical nature of the mounting surface which is not typically parallel. To solve this problem it will probably be necessary to transmit more energy in an expanded arc, reducing the requirement for exact alignment.

The approach to attachment will be to mount the crystals in structures that can be buttoned through the cardiac walls in similar fashion to the technique employed to mount pressure transducers within the cardiac spaces.

DEMODULATORS

Low power electronics necessary to convert frequency modulated information to voltage modulated information have been designed and tested. Figure 7 illustrates the general circuit for such a device. Operation is as follows: Frequency modulated input signals are limited to produce a square wave. The leading edge of the square wave sets a monostable which resets after a prescribed period. As the input frequency changes, the ratio of on time to off time on the monostable output changes. The monostable output is averaged to produce an output directly proportional to the input frequency. Figure 8 illustrates a calibration curve on such a circuit.

24 November 1969

-5-

SUMMARY

The function of the device is not yet optimized. An improved pinger design is probably necessary in order to transmit more energy. The optimum crystal probe design has not yet been achieved. With the current crystal probe design the alignment must be quite exact in order to obtain proper function. In the next two months these two problems will be dealt with.

Original Copy Signed
By John P. Meehan, M.D.

John P. Meehan, M.D.
Principal Investigator

JPM/br

Reference

1. Kardon, Merrill B., Stegall, Hugh F., and Stone, Hubert L.: "A Simple Portable Sonomicrometer". USAF School of Aerospace Medicine, Aerospace Medical Division (AFSC) Brooks Air Force Base, Texas, Report SAM-TR-66-96, p.2, November, 1966.

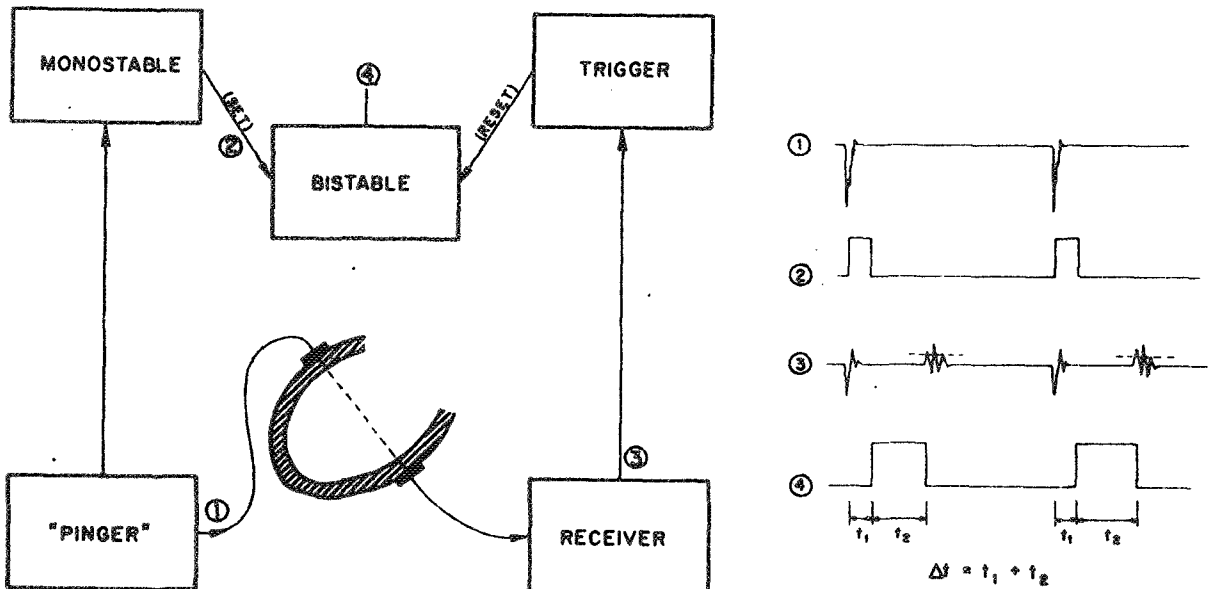


Figure 1. Block diagram with waveforms illustrating the output of each stage:

- (1) "Pinger" pulse which drives the transmitting crystal
- (2) Monostable multivibrator output (trailing edge "sets" the bistable)
- (3) Receiver output showing "pinger" pulse feedthrough and received packet which "resets" the bistable
- (4) Bistable multivibrator output (t_2 varies with transit time)

This figure is from: "A Simple Portable Sonomicrometer" by Merrill B. Kardon, Hugh F. Stegall, and Hubert L. Stone; USAF School of Aerospace Medicine, Aerospace Medical Division (AFSC) Brooks Air Force Base, Texas, Report SAM-TR-66-96, p. 2, November, 1966.

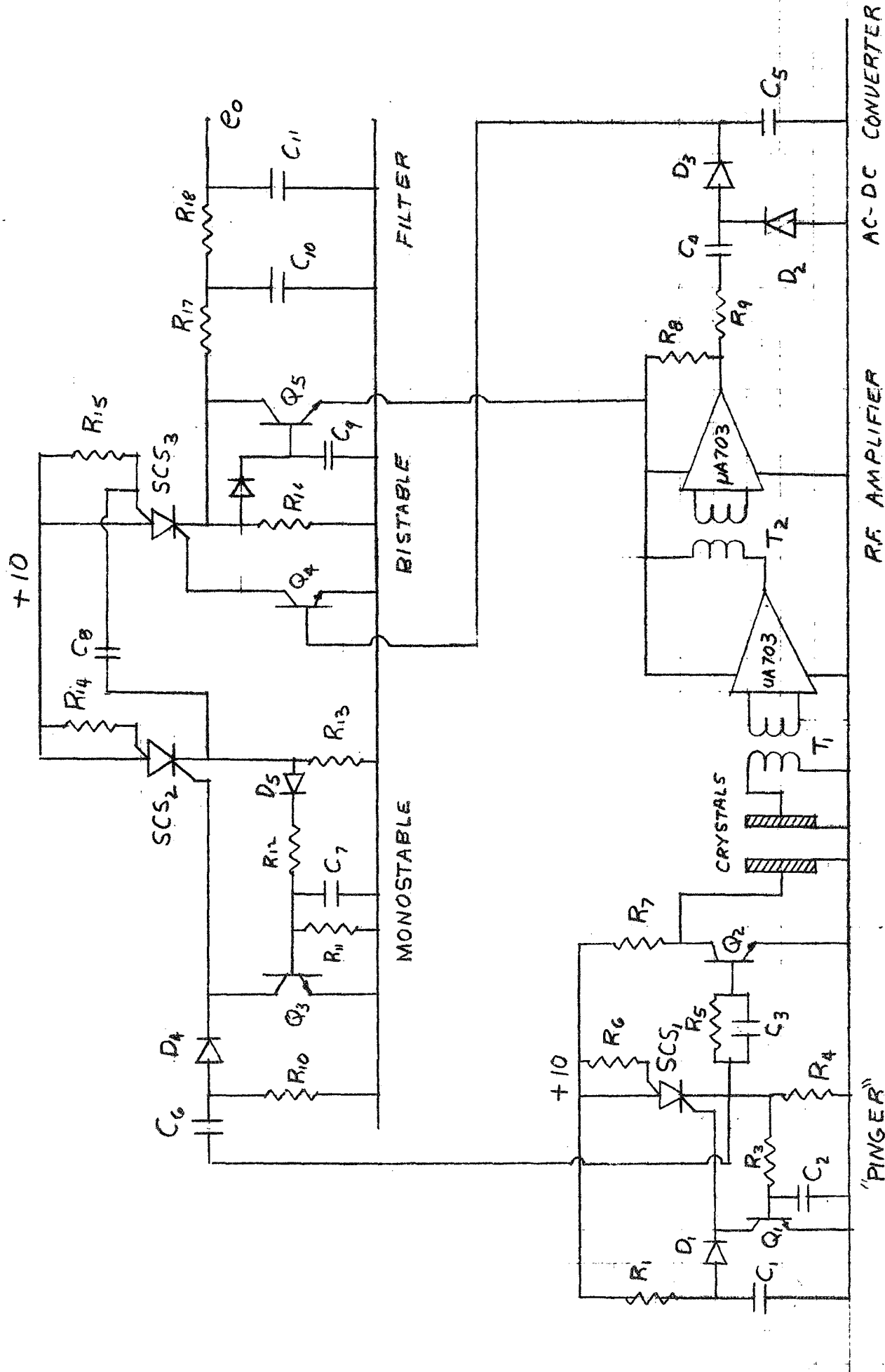


Figure 2. Sonomicrometer Circuit Diagram

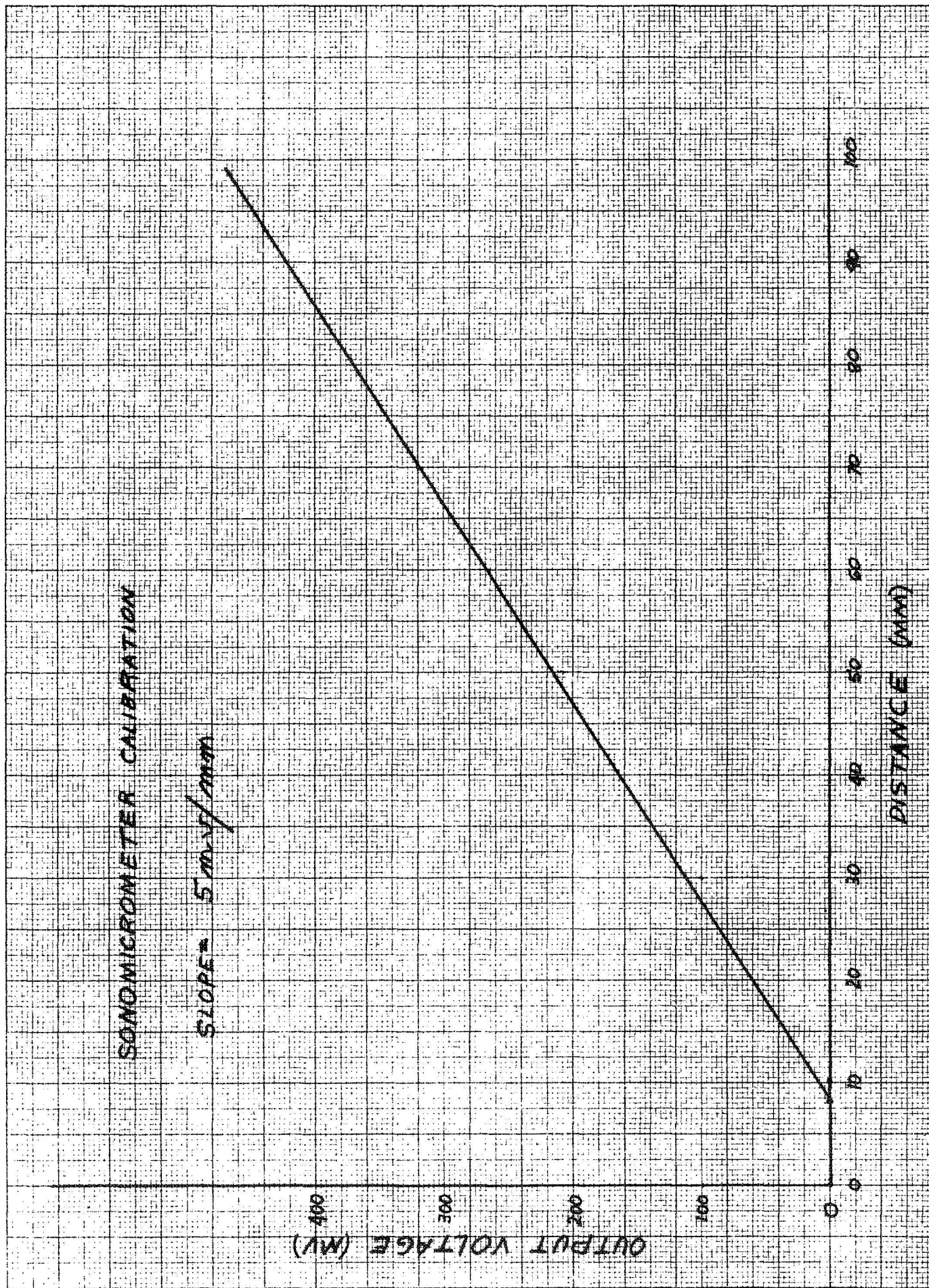


Figure 3. Sonomicrometer Calibration

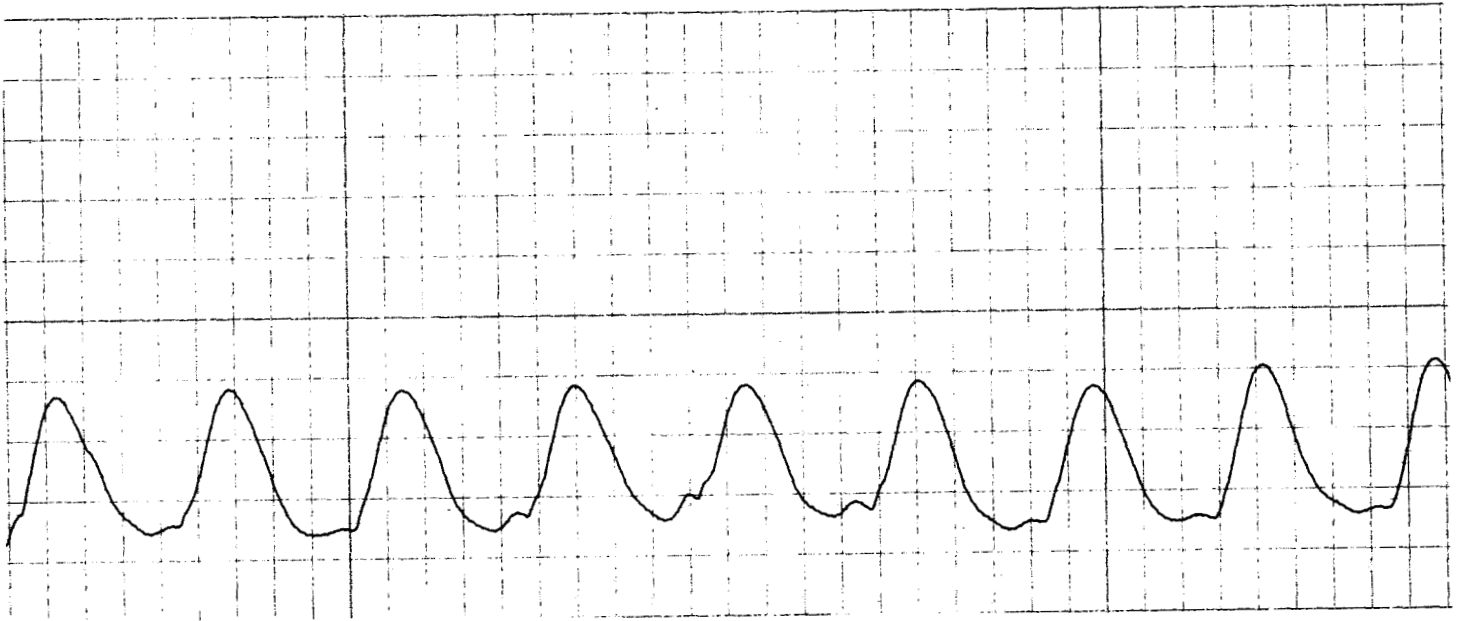


Figure 4. Right Atrium

Time Scale = 50 mm/sec
Sensitivity = 2 mv/div
 Δ Distance = $\frac{24 \text{ mv}}{5 \text{ mv}} \text{ mm} = 5 \text{ mm}$

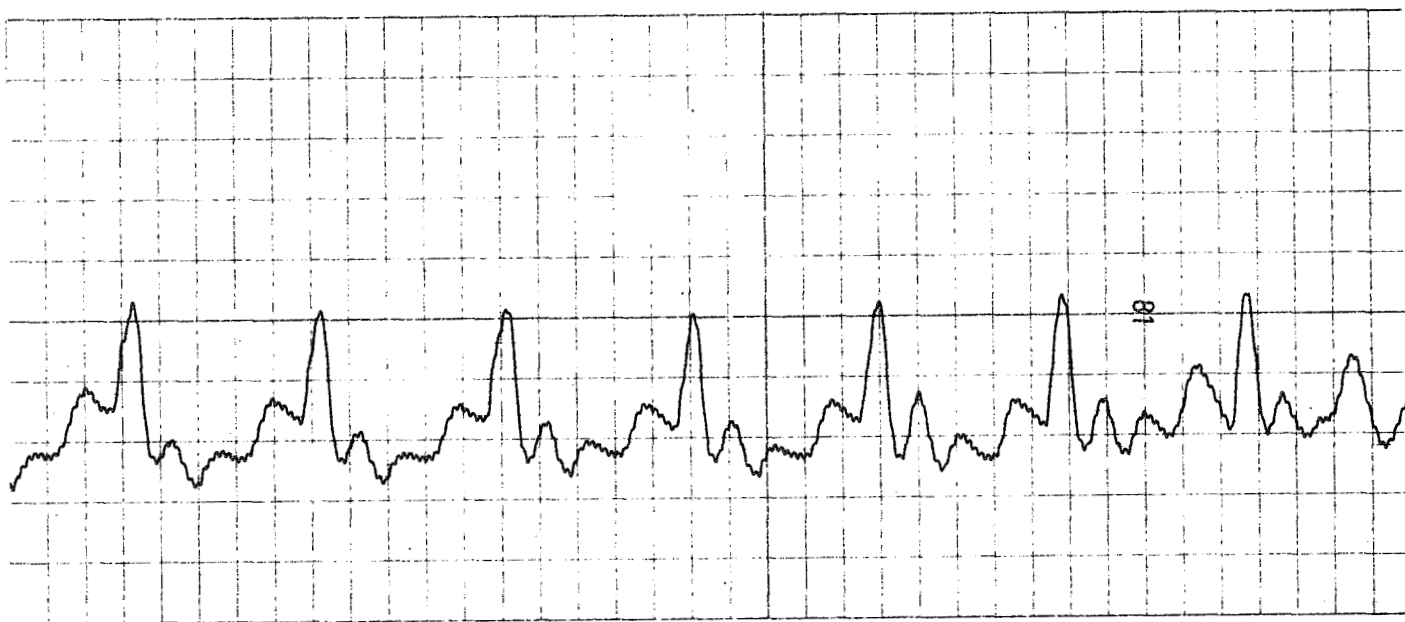


Figure 5. Anterior Vena Cava

Time Scale = 50 mm/sec
Sensitivity = 0.5 mv/div
 Δ Distance = $\frac{7 \text{ mv mm}}{5 \text{ mv}} = 1.4 \text{ mm}$

FIGURE 6
 NONLINEAR CALIBRATION

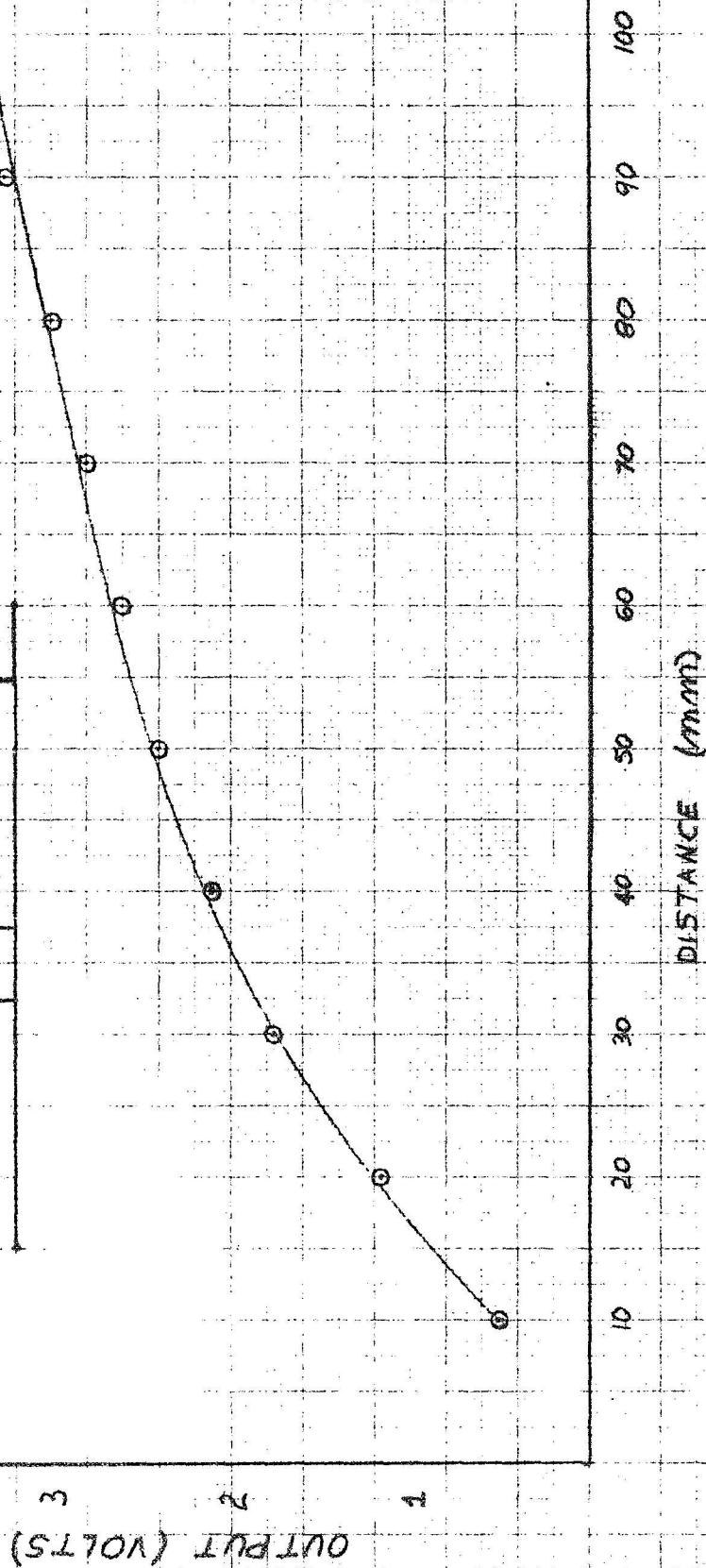
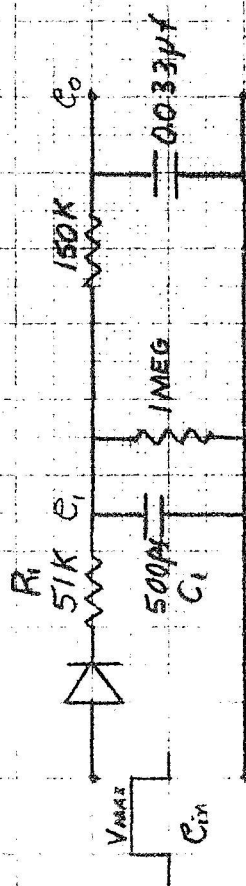


Figure 6. Nonlinear Calibration

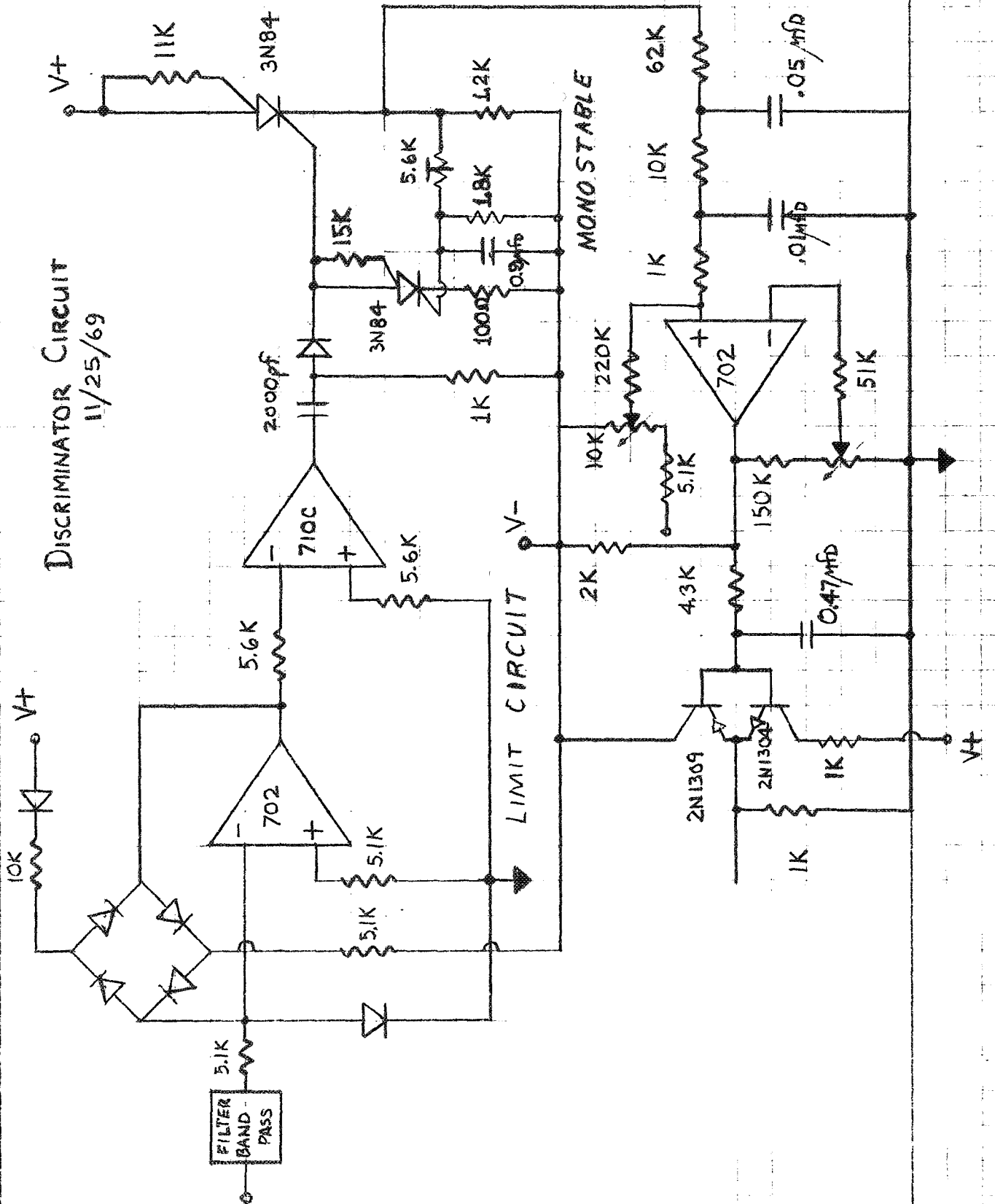


Figure 7. Demodulator Circuit

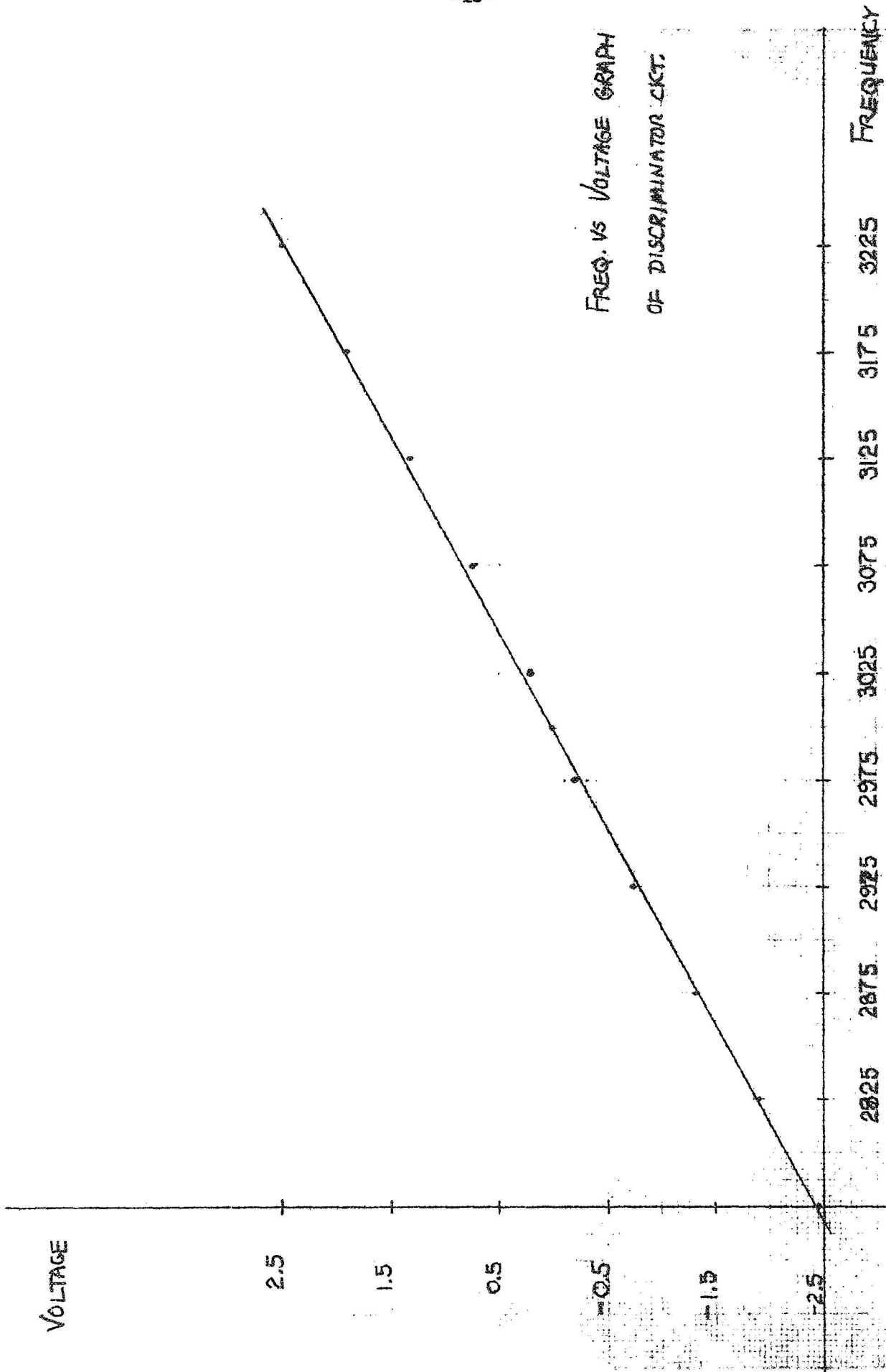


Figure 8. Demodulator Calibration Curve